Available online at www.sciencedirect.com

ScienceDirect

Ceramics International 40 (2014) 3023–3029

CERAMICS INTERNATIONAL

www.elsevier.com/locate/ceramint

Fabrication of multifunctional TiO_2–fly ash/polyurethane nanocomposite membrane via electrospinning

Han Joo Kim[a], Hem Raj Pant[b,c,*], Jun Hee Kim[b], Nag Jung Choi[a,*], Cheol Sang Kim[a,b,**]

[a]Division of Mechanical Design Engineering, Chonbuk National University, Jeonju 561-756, Republic of Korea
[b]Department of Bio-nano System Engineering, Chonbuk National University, Jeonju 561-756, Republic of Korea
[c]Department of Engineering Science and Humanities, Institute of Engineering, Pulchowk Campus, Tribhuvan University, Kathmandu, Nepal

Received 27 August 2013; received in revised form 3 October 2013; accepted 3 October 2013
Available online 10 October 2013

Abstract

In this study, we demonstrate the fabrication of multifunctional composite polyurethane (PU) membrane from a sol gel system containing TiO_2 and fly ash (FA) nanoparticles (NPs). The adsorptive property of FA and photocatalytic property of TiO_2 can introduce different functionalities on PU mat for water purification. Different types of PU nanofiber mats were prepared by varying the composition of NPs in blend solution. FE-SEM, TEM, TGA, XRD, UV–visible spectra, and water contact angle measurement confirmed the incorporation of FA and TiO_2 NPs on/into PU nanofibrous mat. The influence of NPs on PU membrane was evaluated from the adsorption of heavy metals (Hg, Pb), removal of dyes (methylene blue), antibacterial activity, and water flux. The improvement of all these activities is attributed to the adsorptive property of FA and photocatalytic/hydrophilic property of TiO_2 NPs. Therefore, as-synthesized composite membrane can be utilized as an economically friendly filter media for water purification.

Keywords: D. TiO_2; Adsorption; Electrospinning; Fly ash; Polyurethane

1. Introduction

Inorganic/organic nanocomposites (IONCs) have attracted growing attention due to their improved physicochemical properties for different applications. A variety of IONCs with different morphologies can be synthesized by using various methods such as chemical/physical vapor deposition, arc discharge, laser ablation, and electrospinning [1–9]. Among them, electrospining is a simple technique for the production of polymeric nanofibers containing inorganic nanoparticles. In this process, inorganic NPs can be simply blended with polymer solution prior to electrospinning and this sol gel system is allowed to pass through high electric field where electrically driven liquid jet can produce polymeric nanofibers containing inorganic NPs. The unique properties such as high surface area, high aspect ratio, good mechanical properties of electrospun nanofibers and the incorporation of multifunctional inorganic NPs through them can produce excellent filter media for water purification.

In the last few years, a wide range of synthetic polymers have been used to produce pristine and composite nanofibers. Among them PU is a thermoplastic elastomer of significant industrial importance. It possesses a wide range of desirable properties such as good mechanical properties, excellent hydrolytic stability, and resistance to abrasion [10–14]. Electrospun PU nanofibrous mats are widely used in air/water filtration, protective textiles, biomaterials, and sensors [11,15–17]. Therefore, PU nanofibers have been found to be a very promising material of interest. Incorporation of inorganic NPs through PU fibers can broaden its application as such kinds of composite membranes possess unique properties.

Fly ash (FA) is a by-product generated in coal fired power plants and may cause environmental pollution if it is not disposed properly. Its favorable properties such as sphericity, porosity, nontoxicity, lightweight property, and high strength

*Corresponding authors: Tel.: +82 6327 04284; fax: +82 6327 02460.
**Corresponding author at: Division of Mechanical Design Engineering, Chonbuk National University, Jeonju 561-756, Republic of Korea. Tel.: +82 6327 04284; fax: +82 6327 02460.
E-mail addresses: hempant2002@yahoo.com, hempant@jbnu.ac.kr (H. Raj Pant), njchoi@jbnu.ac.kr (N. Jung Choi), chskim@jbnu.ac.kr (C. Sang Kim).

0272-8842/$ - see front matter © 2013 Elsevier Ltd and Techna Group S.r.l. All rights reserved.
http://dx.doi.org/10.1016/j.ceramint.2013.10.005

make it cost effective materials for different applications [11,15,18]. Fly ash has been widely studied in wastewater treatments as a porous low-cost adsorbent to replace costly granular activated carbon [19,20]. These properties of FA can be further improved by incorporating varieties of metal or metal oxide NPs through it [5,20]. Most of the commercially available adsorbent materials are usually obtained in powder or in a granular form, which in many cases constrains their use for practical applications for water treatment. The particle size of the sorbent is small and additional separation system becomes necessary. Therefore, The incorporation of TiO_2 (a well known photocatalyst) and FA NPs (a good adsorbent) through polymer matrix can produce stable and reusable material for water treatment. Their properties can be improved by incorporating them into PU fibers because increasing surface-area-to volume ratio may provide a sufficient area for interaction without agglomeration of NPs during water treatment.

In this study, we prepared TiO_2 and FA NPs incorporated PU composite nanofibers using electrospinning of blend of these materials. Pristine PU, FA/PU, TiO_2/PU and TiO_2–FA/PU composite nanofibrous membranes were fabricated. The physicochemical properties of as-fabricated fibers were analyzed by field scanning electron microscopy (FE-SEM), X-ray diffraction (XRD), ultra-violet–visible (UV–vis) spectroscopy, thermo-gravimetric (TGA) analysis, and water contact angle measurement. The improved properties of composite mat compared to the pristine PU were evaluated for heavy metal adsorption, dyes adsorption/degradation, antibacterial capacity, and water flux.

2. Experimental

2.1. Materials

Commercial-grade polyurethane (PU) pellets (Estane® Skythane® X595A-11, Lubrizol Advanced Materials, Inc., USA), TiO_2 NPs (Aeroxide P25, 80%anatase 20% rutile, average particle size of 21 nm and specific surface area $50 \pm 15\ m^2\ g^{-1}$), and the purified fly ash particles (FAPs) (from Won Engineering Company Ltd., Gunsan, Korea) were used for the fabrication of composite nanofibers. N, N dimethylformamide (DMF) (Showa, Japan) and methyl ethyl ketone(2-butanone) (MEK) (Junsei, Japan), $HgCl_2$ (99.5%, Sigma-Aldrich, India) and $Pb(NO_3)_2$ (99.0%, Sigma-Aldrich, Japan) were used as-received.

2.2. Preparation of composite electrospun mats

FAPs (ball-milled using 3 mm zirconia balls and sieved for 12 h) and PU pellets were dried for 3 h in oven at 80 °C prior to dissolution in solvents. Pure PU solution was prepared by dissolving 10 wt% PU in DMF/MEK (50:50 by weight) solvent system and stirring for 10 h using magnetic stirrer. Blend solutions containing 25 wt% FA, 3 wt% TiO_2, and 3 wt% TiO_2 plus 25 wt% FA were prepared using a magnetic stirrer (10 h) followed by ultrasonication (2 h). The prepared solution was placed in a syringe tube and fed through a nozzle with a diameter of 0.25 mm to get a fibrous mat on a polyethylene-sheet-coated rotating drum. Electrospinning was carried out at an applied voltage of 20 kV, tip-to-collector distance of 18 cm, and a solution feed rate of 0.5 ml/h at room temperature. Temperature and humidity were 28% and 39%, respectively. As-fabricated electrospun nanofibrous mats were placed in vacuum being dried for 12 h at 30 °C and were used for further analysis.

2.3. Characterization of electrospun nanofibers

The surface morphologies of different electrospun fibers were analyzed by field emission scanning electron microscopy (FE-SEM, S-7400, Hitachi, Japan). The incorporation of TiO_2 and FAPs into/on PU fibers were evaluated using XRD analysis (Rigaku X-ray diffractometer), thermo-gravimetric analysis (TGA, Perkin-Elmer, USA), and UV–visible spectrometer (Lambda 900, Perkin-Elmer, USA). The wettability of the electrospun mats was measured with deionized water contact angle measurements using a contact angle meter (GBX, Digidrop, France). Deionized water was automatically dropped (drop diameter 6 μm) onto the mat.

2.4. Antibacterial property test

The antibacterial activity of different mats was tested against *Escherichia coli (E. coli)*. The antibacterial experiments were carried out in a sterilized glass beaker containing an *E. coli* suspension (50 ml) with different mats (3 cm × 3 cm). The initial *E. coli* concentration was cultivated at about 10^7 CFU/ml, which was incubated at 37 °C for 12 h in dark and the tests were performed at room temperature for 3 h. The UV light intensity of 1.1 W/cm^2 using a mercury vapor lamp (OmniCure, EXFO) was passed through the system. The use of low strength UV-light (1.1 W/cm^2) can prevent from the fast degradation of PU caused by UV radiation. At specific time intervals, 1 ml of the solution was extracted and immediately spread on Tryptic Soy agar plates. Petrifilm (3 M Petrifilm, USA) and agar plates were prepared to count bacterial colonies. After 24 h of incubation at 37 °C, the number of viable *E. coli* colonies was counted using a colony counter.

2.5. Adsorption of heavy metals

As-synthesized membranes (50 mm × 50 mm in dimension) were used in adsorption experiments for the removal of mercury (II) and lead (II) from synthetic aqueous solution. The aqueous solutions were prepared by dissolving the appropriate amount of $HgCl_2$ (10 ppm) and $Pb(NO_3)_2$ (5 ppm) salts in water. All experiments were carried out in Petri dish containing 50 ml of salt solution with different mat. The progress of adsorption was monitored by determination of the concentration of metallic ions in solution after sampling (aliquot of 5 ml) at specific intervals of time (3 h and 24 h) by means of an inductively coupled plasma mass spectrometer (ICP-MS; Agilent 7500a, USA).

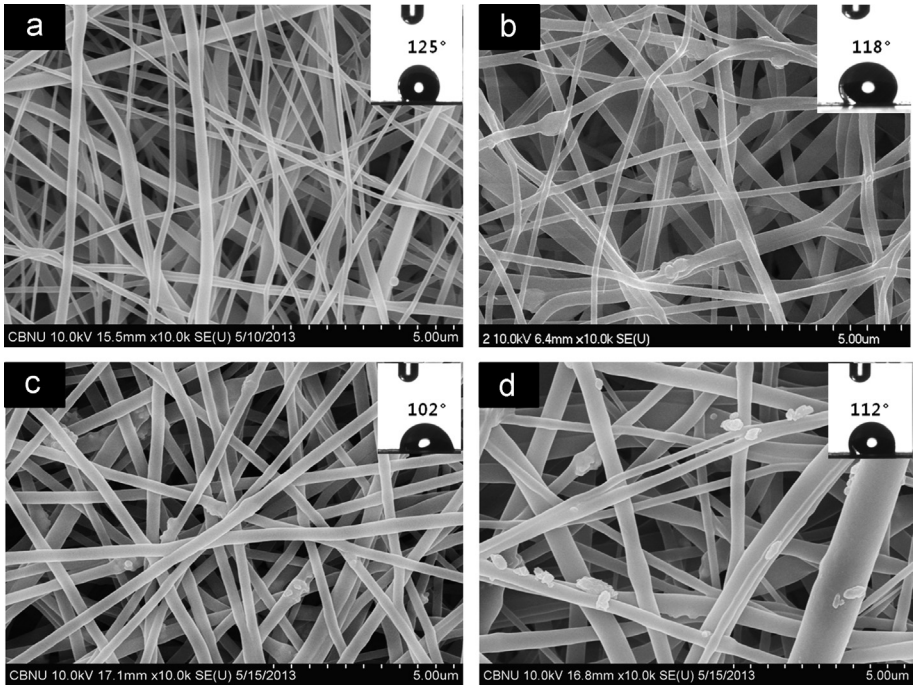

Fig. 1. FE-SEM images of pure PU (a), FA/PU (b), TiO_2/PU (c), and TiO_2–FA/PU (d) mats. Insets are their corresponding contact angles after 9 s on the surface of mats.

2.6. Dye adsorption/degradation test

Dye adsorption/degradation capacity of as-prepared membranes was evaluated using aqueous methylene blue (MB) solution. In the present investigation, the reactions were carried out in Petri dishes under UV-irradiation. 35 ml of dye (10 ppm concentration) was treated with different mats (approximately the same dimension). The samples were taken at regular intervals of time, and the concentration of the dye was measured by recording its absorbance at 663 nm with a UV–visible spectrophotometer (HP 8453 UV–vis spectroscopy system, Germany).

2.7. Water permeability test

For the water permeability test, circular electrospun membranes of 44.5 mm in diameter with an effective area of 13.4 cm^2 were used applying Amicon stirred cell model 8050 [21]. The nitrogen gas was used to supply pressure to the feed water and filter efficiency of membrane was compared by measuring the time required to pass equal volume of pure water through different membranes under similar condition. Four different pressures (0, 5, 10, and 20 psig) were used in this measurement.

3. Results and discussion

The effect of different amounts of FA on fiber morphology was explained in our resent report which showed that 30 wt% FA containing PU solution is the best combination for the fabrication of FA/PU composite fibers [11]. Therefore, we assume that 25 wt% FA and 3 wt% TiO_2 in PU solution might be suitable for the fabrication of TiO_2–FA/PU composite fibers. The morphology of the electrospun PU nanofibrous mats with different combination of inorganic NPs are shown in Fig. 1. Pure PU mat showed bead-free and smooth nanofibers with an average diameter of 354 ± 22 nm, while the composite mats showed thinner nanofiber. The average diameter of FA/PU, TiO_2/PU, and TiO_2–FA/PU nanofibers were 302 ± 23 nm, 310 ± 25 nm, and 320 ± 35 nm, respectively. The cause of decrease in fiber diameter of composite fibers was explained in our previous work [11]. The addition of FA/TiO_2 NPs in PU solution led the increase in solution conductivity and consequently decreases the fiber diameter [11]. FA containing fibers exhibited the effectively embedded NPs through the surface. However, TiO_2 and TiO_2/FA containing fibers showed that large number of particles were also present on the surface of the fibers. It indicated that FA particles have better affinity towards PU compare to TiO_2 NPs. Our previous results showed that sufficient amount of FA (up to 70 wt%) can be incorporated through polymer fibers [11], while large amount of TiO_2 cannot be incorporated through polymer fibers during electrospinning [21,22].

Effective incorporation of inorganic NPs through polymer matrix was further supported by XRD, and UV–visible spectroscopy. The XRD patterns of pure PU, FA/PU, TiO_2/PU, and TiO_2–FA/PU fibers are shown in Fig. 2. It shows similar XRD pattern as was reported in our previous result [11] for PU and FA/PU membrane. FA/PU membrane demonstrates the existence of mullite (card no. 150776) and quartz crystal [23]. The presence of characteristic peaks of anatase and rutile phase of TiO_2 are clearly observed in composite TiO_2/PU fibers which are in exactly same patterns as observed in TiO_2/nylon-6 fibers of our previous report [22]. The corresponding peaks of FA and TiO_2 are clearly seen on TiO_2–FA/PU mat and indicate the incorporation of these inorganic NPs through

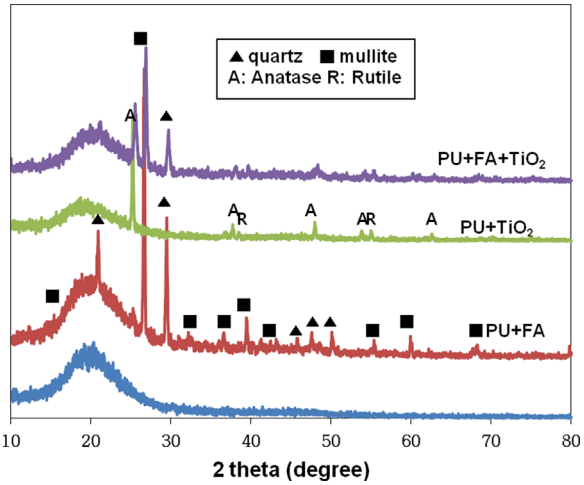

Fig. 2. XRD patterns of different mats.

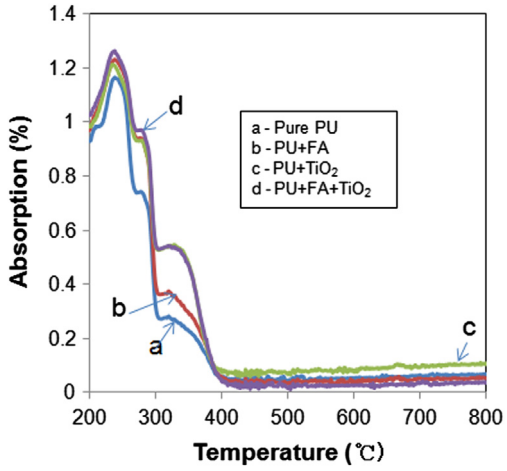

Fig. 3. UV–visible absorption spectra of pure PU (a), FA/PU (b), TiO_2/PU (c), and TiO_2–FA/PU (d) mats.

polymer matrix. The incorporation of TiO_2 NPs through composite fibers was also confirmed by UV–visible spectra. Fig. 3 shows the UV–visible absorption spectra of the electrospun pure PU fibers and those of the three different composite PU fibers containing inorganic NPs. The absorption band of TiO_2 below 400 nm is pronounced in the composite mats containing TiO_2 and TiO_2–FA NPs. The UV–visible spectra not only show the presence of TiO_2 NPs on the fiber but also indicate the use of nanocomposite membrane for UV protecting textile. It shows that this composite textile material can absorb UV radiation which prevent from passing UV radiation through it and reach up to the human body.

The incorporation of inorganic NPs through PU fibers was also confirmed via thermo-gravimetric analysis (TGA) which is shown in Fig. 4. In this figure, one can see the initial thermal degradation of each mats is started from about 300 °C and completed at about 400 °C which shows the thermal degradation of PU fibers [24]. Inorganic NPs-free PU mat is thermally more stable than the hybrid mats. The maximum thermal decomposition temperature of pristine PU fibers is 345 °C where as this value for FA/PU, TiO_2/PU, and TiO_2–FA/PU

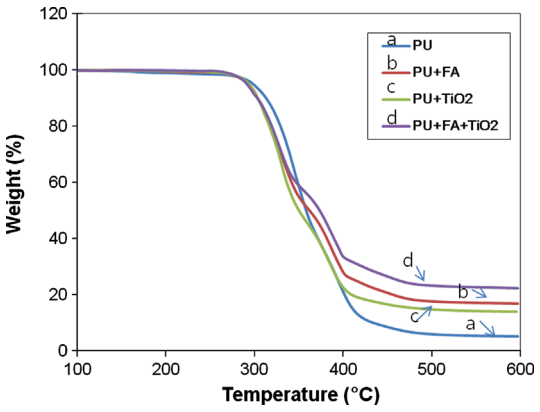

Fig. 4. TGA curves for pure PU (a), FA/PU (b), TiO_2/PU (c), and TiO_2–FA/PU (d) mats.

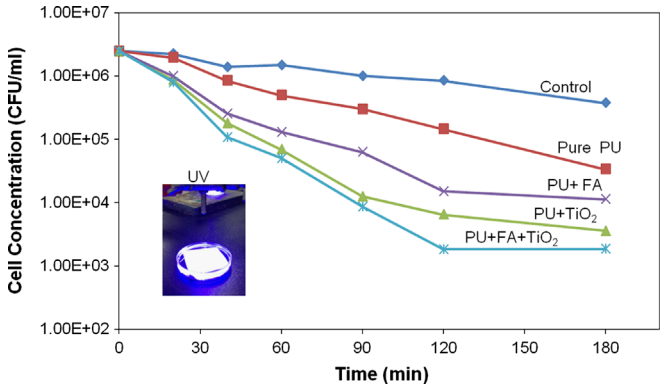

Fig. 5. Antibacterial efficiency of different mats on *E. coli* bacteria under UV radiation.

composite fibers is 327, 330, and 328 °C, respectively. Similarly, overall weight loss of different mats is in the order of PU < TiO_2/PU < FA/PU < TiO_2–FA/PU which is in the good agreement with the initial amount of NPs added into the electrospinning solution.

Our aim is the fabrication of unique multifunctional membrane where single mat posses different properties to remove the verities of contaminants present in water. Fly ash and PU are good adsorbent where as TiO_2 is excellent photocatalyst. Therefore, the combination of these three materials as a nanocomposite fiber can provide an excellent filter media for water purification. The antibacterial capacity of as-synthesized mats was evaluated under mild UV radiation and result is presented in Fig. 5. The figure clearly indicates the better antibacterial capacity of TiO_2 NPs containing PU fibers compared to the TiO_2-free fibers. The antibacterial effect of FA/PU composite membrane is effectively increased when small amount of TiO_2 is incorporated through it. The photocatalytic activity of TiO_2 semiconductor under UV irradiation is well known for the destruction of bacteria [25,26]. Therefore, TiO_2–FA/PU membrane can be used as a good antibacterial filter media for water purification.

The adsorption/photocatalytic degradation performance of the as-synthesized mats was evaluated by adsorbing/degrading methylene blue (MB) under UV-light irradiation. It was clear

from Fig. 6 that the FA/PU and TiO_2/PU composite mats have good capacity to remove dye from water. The dye removable capacity of FA/PU composite is due to the good adsorption capacity of FA particles [15,27,28] where as improved dye removable capacity of TiO_2–FA/PU composite is due to the photocatalytic activity of TiO_2 NPs. The highest dye removable capacity of TiO_2–FA/PU composite is due to the combined effect of adsorption (caused by FA) and phytocatalytic degradation (caused by TiO_2). The result is related to the role of FA on the surface of PU fibers. Here, adsorbed dye molecules on the surface of composite fibers (caused by FA) were photodegraded by TiO_2 and adsorption process never becomes saturated. FA particles continuously adsorb dye molecules which are subsequently photodegraded by TiO_2 NPs.

Fly ash is highly used for the adsorption of heavy metals [29–33]. Therefore, PU composite membrane containing FA particles can be considered as a good adsorbent of heavy metals. This capacity of composite membrane was experimentally investigated using aqueous solution containing Hg and Pb ions. Fig. 7 presents the removal of Hg and Pb by the different membranes which indicates that FA/PU composite mat has the highest adsorption capacity towards heavy metals. The adsorption performance of TiO_2–FA/PU mat exhibited a lower effect compared to that of FA/PU mat because of the deposition of small TiO_2 NPs on the surface of big FA particles which may block the adsorption site of FA. FE-SEM image clearly revealed that TiO_2 NPs are deposited on the surface of the fibers (Fig. 1c and d) whereas FA particles are effectively embedded through the fibers (Fig. 1b). Therefore, presence of TiO_2 NPs on the surface of composite mat may block the adsorption sites of FA and consequently decrease the adsorption efficiency of the mat. From Fig. 7, it is clear that the adsorbed amount of Pb is higher in FA/PU or TiO_2–FA/PU composite mats compared to the amount of Hg adsorbed by the same mat. Furthermore, Fig. 7 indicates that the sufficient amount of Pb is adsorbed by composite mat within 3 h whereas adsorption of Hg is continued up to 24 h. The better adsorption efficiency of as-synthesized composite membrane towards Pb compared to Hg is due to the different affinity of formation of MOH^+ cations of these two metals [34]. Both Pb and Hg could form MOH^+ cations in water, however, greater affinity of Pb ion (from highly soluble $Pb(NO_3)_2$) to form $PbOH^+$ cation compared to the formation affinity of $HgOH^+$ cation (from less soluble $HgCl_2$) led the better adsorption of Pb, which was also reported in the literatures [31,34].

The filtration efficiency of as-synthesized membranes was studied using Amicon stirred cell model 8050. The pure water flux of different membranes is given in Fig. 8. From the figure, it is clear that the order of water flux is PU > FA/PU < TiO_2/PU > TiO_2–FA/PU. The slightly less value of water flux of composite FA/PU membrane compared to the pristine PU might be due the deposition of NPs on the surface of the fibers which may decrease the pore size of the membrane. However, more water flux of TiO_2/PU and TiO_2–FA/PU composite

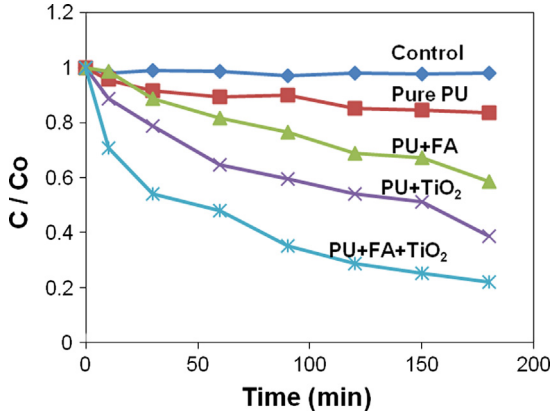

Fig. 6. Comparison of MB photodegradation of different specimens under UV light.

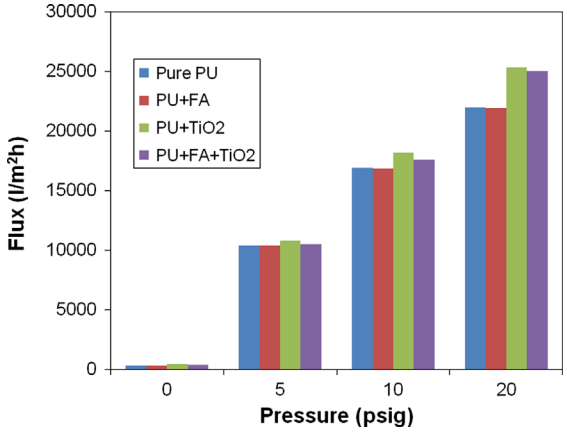

Fig. 8. Water permeation flux of different mats.

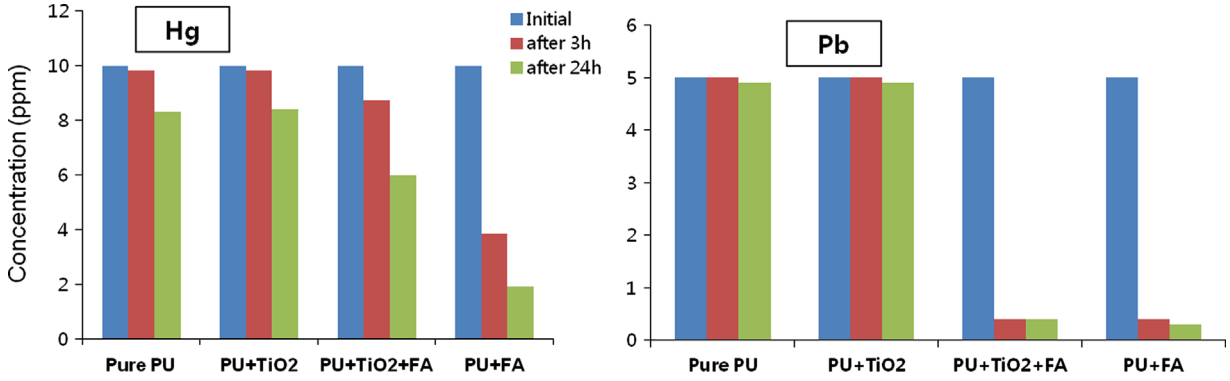

Fig. 7. Hg and Pb adsorption capacity of PU different mats.

compare to pristine PU membrane is due to the increased hydrophilicity of the membranes (See inset of Fig. 1).

4. Conclusions

TiO_2–FA/PU composite multifunctional membrane is successfully developed using eco-friendly facile one-step electrospinning process for water purification. Observed physicochemical properties (FE-SEM, XRD, TGA, and UV–visible spectra) showed that TiO_2 and FAPs were incorporated through the polymer matrix. The adsorptive properties of FA and photocatalytic properties of TiO_2 can induce the different functionalities to the composite membrane. The antibacterial, photocatalytic, and adsorption properties of composite membrane were evaluated using bacteria, dye, and heavy metals/dye, respectively. Preliminary observations used for above mentioned applications showed that it will be an economically and environmentally friendly nonwoven matrix for water purification.

Acknowledgments

We acknowledge the research funds supported by the Korean Ministry of Education, Science and Technology (MEST) through the National Research Foundation (NRF) (Project no. 2013R1A2A2A04015484) and a Grant for first step business project funded by the Korean small and medium business administration (Project no. C0114366). We would also like to thank KBSI, Jeonju branch for FE-SEM images.

References

[1] N.A.M. Barakat, M.F. Abadir, F.A. Sheikh, M.A. Kanjwal, S.J. Park, H.Y. Kim, Polymeric nanofibers containing solid nanoparticles prepared by electrospinning and their applications, Chem. Eng. J. 156 (2) (2010) 487–495.

[2] N. Bhardwaj, S.C. Kundu, Electrospinning: a fascinating fiber fabrication technique, Biotechnol. Adv. 28 (3) (2010) 325–347.

[3] S. Agarwal, A. Greiner, J.H. Wendorff, Functional materials by electrospinning of polymers, Prog. Polym. Sci. 38 (6) (2013) 963–991.

[4] R. Dastjerdi, M. Montazer, A review on the application of inorganic nano-structured materials in the modification of textiles: focus on antimicrobial properties, Colloid Surf. B 79 (1) (2010) 5–18.

[5] V. Beachley, X.J. Wen, Polymer nanofibrous structures: Fabrication, biofunctionalization, and cell interactions, Prog. Polym. Sci. 35 (7) (2010) 868–892.

[6] B. Gong, J.C. Spagnola, S.A. Arvidson, S.A. Khan, G.N. Parsons, Directed inorganic modification of bi-component polymer fibers by selective vapor reaction and atomic layer deposition, Polymer 53 (21) (2012) 4631–4636.

[7] L. Ma, A. Chen, J. Lu, Z. Zhang, H. He, C. Li, In situ synthesis of CNTs/Fe–Ni/TiO2 nanocomposite by fluidized bed chemical vapor deposition and the synergistic effect in photocatalysis, Particuology (0).

[8] V. Eskizeybek, F. Sarı, H. Gülce, A. Gülce, A. Avcı, Preparation of the new polyaniline/ZnO nanocomposite and its photocatalytic activity for degradation of methylene blue and malachite green dyes under UV and natural sun lights irradiations, Appl. Catal. B: Environ. 119–120 (0) (2012) 197–206.

[9] P. Wagener, S. Faramarzi, A. Schwenke, R. Rosenfeld, S. Barcikowski, Photoluminescent zinc oxide polymer nanocomposites fabricated using picosecond laser ablation in an organic solvent, Appl. Surf. Sci. 257 (16) (2011) 7231–7237.

[10] L.D. Tijing, C.-H. Park, S.-J. Kang, A. Amarjargal, T.-H. Kim, H.R. Pant, H.J. Kim, D.H. Lee, C.S. Kim, Improved mechanical properties of solution-cast silicone film reinforced with electrospun polyurethane nanofiber containing carbon nanotubes, Appl. Surf. Sci. 264 (0) (2013) 453–458.

[11] H.J. Kim, H.R. Pant, N.J. Choi, C.S. Kim, Composite electrospun fly ash/polyurethane fibers for absorption of volatile organic compounds from air, Chem. Eng. J. 230 (0) (2013) 244–250.

[12] V. Acharya, C. Ratna Prabha, C. Narayanamurthy, Synthesis of metal incorporated low molecular weight polyurethanes from novel aromatic diols, their characterization and bactericidal properties, Biomaterials 25 (19) (2004) 4555–4562.

[13] P. Russo, D. Acierno, G. Marletta, G.L. Destri, Tensile properties, thermal and morphological analysis of thermoplastic polyurethane films reinforced with multiwalled carbon nanotubes, European Polymer Journal (0).

[14] H. Keskin, A. Tekin, Abrasion resistances of cellulosic, synthetic, polyurethane, waterborne and acidhardening varnishes used woods, Constr. Build. Mater. 25 (2) (2011) 638–643.

[15] M. Visa, C. Bogatu, A. Duta, Simultaneous adsorption of dyes and heavy metals from multicomponent solutions using fly ash, Appl. Surf. Sci. 256 (17) (2010) 5486–5491.

[16] J. Lee, E.J. Park, J. Choi, J. Hong, S.E. Shim, Polyurethane/PEG-modified MWCNT composite film for the chemical vapor sensor application, Synth. Met. 160 (7–8) (2010) 566–574.

[17] X. Hu, M. Zhang, W. Ruan, F. Zhu, G. Ouyang, Determination of organophosphorus pesticides in ecological textiles by solid-phase microextraction with a siloxane-modified polyurethane acrylic resin fiber, Anal. Chim. Acta 736 (0) (2012) 62–68.

[18] P. Sultana, S. Das, A. Bhattacharya, R. Basu, P. Nandy, Development of iron oxide and titania treated fly ash based ceramic and its bioactivity, Mater. Sci. Eng. C-Mater. 32 (6) (2012) 1358–1365.

[19] T. Lindgren, D. Norback, Cabin air quality: indoor pollutants and climate during intercontinental flights with and without tobacco smoking, Indoor Air 12 (4) (2002) 263–272.

[20] M. Ahmaruzzaman, Role of fly ash in the removal of organic pollutants from wastewater, Energy Fuel 23 (2009) 1494–1511.

[21] H.R. Pant, B. Pant, P. Pokharel, H.J. Kim, L.D. Tijing, C.H. Park, D.S. Lee, H.Y. Kim, C.S. Kim, Photocatalytic TiO_2–RGO/nylon-6 spider-wave-like nano-nets via electrospinning and hydrothermal treatment, J. Membr. Sci. 429 (0) (2013) 225–234.

[22] H.R. Pant, M.P. Bajgai, K.T. Nam, Y.A. Seo, D.R. Pandeya, S.T. Hong, H.Y. Kim, Electrospun nylon-6 spider-net like nanofiber mat containing TiO_2 nanoparticles: a multifunctional nanocomposite textile material, J. Hazardous Mater. 185 (1) (2011) 124–130.

[23] Y.N. Yang, H.X. Zhang, P. Wang, Q.Z. Zheng, J. Li, The influence of nano-sized TiO_2 fillers on the morphologies and properties of PSFUF membrane, J. Membr. Sci 288 (1–2) (2007) 231–238.

[24] B.B. Khatua, C.K. Das, Effect of processing on the thermal stability of blends based on polyurethane, Part I, Polym. Degrad. Stab. 69 (3) (2000) 381–386.

[25] Y. Zhang, Y.F. Wu, M. Chen, L.M. Wu, Fabrication method of TiO_2–SiO_2 hybrid capsules and their UV-protective property, Colloid Surf. A 353 (2–3) (2010) 216–225.

[26] J. Kiwi, V. Nadtochenko, Evidence for the mechanism of photocatalytic degradation of the bacterial wall membrane at the TiO_2 interface by ATR-FTIR and laser kinetic spectroscopy, Langmuir 21 (10) (2005) 4631–4641.

[27] C.W. Purnomo, C. Salim, H. Hinode, Effect of the activation method on the properties and adsorption behavior of bagasse fly ash-based activated carbon, Fuel Process. Technol. 102 (0) (2012) 132–139.

[28] X.-W. Wu, H.-W. Ma, L.-T. Zhang, F.-J. Wang, Adsorption properties and mechanism of mesoporous adsorbents prepared with fly ash for removal of Cu(II) in aqueous solution, Appl. Surf. Sci. 261 (0) (2012) 902–907.

[29] M. Liu, L.-A. Hou, B. Xi, Y. Zhao, X. Xia, Synthesis, characterization, and mercury adsorption properties of hybrid mesoporous aluminosilicate sieve prepared with fly ash, Appl. Surf. Sci. 273 (0) (2013) 706–716.

[30] E. Sočo, J. Kalembkiewicz, Adsorption of nickel(II) and copper(II) ions from aqueous solution by coal fly ash, Journal of Environmental Chemical Engineering (0).
[31] A.D. Papandreou, C.J. Stournaras, D. Panias, I. Paspaliaris, Adsorption of Pb(II), Zn(II) and Cr(III) on coal fly ash porous pellets, Miner. Eng. 24 (13) (2011) 1495–1501.
[32] J.C. Hower, C.L. Senior, E.M. Suuberg, R.H. Hurt, J.L. Wilcox, E.S. Olson, Mercury capture by native fly ash carbons in coal-fired power plants, Prog. Energy Combust. 36 (4) (2010) 510–529.
[33] J.F. Pang, Q. Li, B. Wang, D.J. Tao, X.T. Xu, W. Wang, J.P. Zhai, Preparation and characterization of electroless Ni–Fe–P alloy films on fly ash cenospheres, Powder Technol. 226 (2012) 246–252.
[34] E.P. Kuncoro, M.Z. Fahmi, Removal of Hg and Pb in aqueous solution using coal Fly Ash adsorbent, Procedia Earth Planet. Sci. 6 (0) (2013) 377–382.